

Can MLLMs Guide Weakly-Supervised Temporal Action Localization Tasks?

Quan Zhang¹ Yuxin Qi²

¹Tsinghua University, Beijing, China

²Shanghai Jiao Tong University, Shanghai, China

zhangqua22@mails.tsinghua.edu.cn, qiyuxin98@sjtu.edu.cn

Abstract

Recent breakthroughs in Multimodal Large Language Models (MLLMs) have gained significant recognition within the deep learning community, where the fusion of the Video Foundation Models (VFM) and Large Language Models (LLMs) has proven instrumental in constructing robust video understanding systems, effectively surmounting constraints associated with predefined visual tasks. These sophisticated MLLMs exhibit remarkable proficiency in comprehending videos, swiftly attaining unprecedented performance levels across diverse benchmarks. However, their operation demands substantial memory and computational resources, underscoring the continued importance of traditional models in video comprehension tasks. In this paper, we introduce a novel learning paradigm termed MLLM4WTAL. This paradigm harnesses the potential of MLLM to offer temporal action key semantics and complete semantic priors for conventional Weakly-supervised Temporal Action Localization (WTAL) methods. MLLM4WTAL facilitates the enhancement of WTAL by leveraging MLLM guidance. It achieves this by integrating two distinct modules: Key Semantic Matching (KSM) and Complete Semantic Reconstruction (CSR). These modules work in tandem to effectively address prevalent issues like incomplete and over-complete outcomes common in WTAL methods. Rigorous experiments are conducted to validate the efficacy of our proposed approach in augmenting the performance of various heterogeneous WTAL models.

Introduction

Temporal action localization (TAL) (Paul, Roy, and Roy-Chowdhury 2018; Narayan et al. 2021; Lee et al. 2021; Alayrac et al. 2022; Dai et al.) aims to localize action instances of interest from untrimmed videos. Although current fully-supervised TAL methods achieve significant localization results, fully-supervised methods require expensive, time-consuming, and labor-intensive frame-level annotations, and weakly-supervised temporal action localization (WTAL) methods (Paul, Roy, and Roy-Chowdhury 2018; Narayan et al. 2021; Lee et al. 2021), which require only video-level labels, have received much attention in order to alleviate the cost of annotation.

Existing WTAL methods typically train a classifier (Paul, Roy, and Roy-Chowdhury 2018; Narayan et al. 2021; Lee et al. 2021) using video-level labels, generating a set of

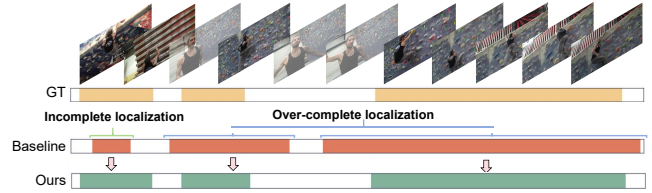


Figure 1: Previous methods have problems of over-complete positioning and incomplete positioning.

probability predictions. This process results in temporal class activation maps (T-CAM). Despite notable performance improvements, current methods still face two challenges: incomplete and over-complete localization. As illustrated in Fig.1, some sub-actions with low discriminability may be ignored, leading to incomplete localization, while certain background segments that contribute to classification might be misclassified as foreground actions, causing over-complete localization.

To overcome these challenges, we turn our perspective to existing multimodal large language models (MLLMs) (Alayrac et al. 2022; Dai et al.). The state-of-the-art MLLM employs a seamless amalgamation of a video foundation model and a large language model, culminating in the development of a sophisticated system for enhanced video comprehension. This integrated framework transcends the limitations inherent in traditional predefined visual tasks. Although MLLM exhibits powerful video understanding capabilities, the resource-intensive nature of running it poses high memory and computational costs. Therefore, traditional models remain essential for video understanding tasks. Is it possible to propose a learning paradigm that leverages MLLMs to enhance existing traditional WTAL methods? Inspired by this, we introduce a paradigm for MLLM-enhanced WTAL tasks, known as MLLM4WTAL.

Aiming at the incomplete and over-complete localization problems of previous WTAL methods, we propose MLLM-based key semantic matching (KSM) and complete semantic reconstruction (CSR) modules. KSM aims to utilize MLLM to generate key semantic priors for videos, matching segments in the video based on key semantic embeddings and video embeddings. This matching strategy helps locate key

intervals for temporal actions. CSR aims to utilize MLLM to generate complete semantic priors for videos. By reconstructing the complete semantics of masked action words, we aim to mine the time interval of action instances as complete as possible. This reconstruction strategy helps locate complete intervals for temporal actions.

Based on KSM and CSR, we obtain the key intervals and the complete intervals of the temporal action in turn. Due to the task characteristics of KSM, it may overly focus on segments most matching key semantics, neglecting fewer matching segments, leading to incomplete localization. On the other hand, due to the task characteristics of CSR, it may associate as many segments as possible with key action verbs, often introducing background segments similar to foreground actions, resulting in over-complete localization. Considering the strengths and weaknesses of the two modules, we propose a dual prior interactive enhancement optimization strategy. First, the KSM branch performs forward operations to obtain \mathcal{A}_{KSM} , and then the CSR branch uses \mathcal{A}_{KSM} as the optimization target to alleviate its over-complete localization problem. Subsequently, the CSR branch performs forward operations to obtain \mathcal{A}_{CSR} , and then the KSM branch uses \mathcal{A}_{CSR} as the optimization target to alleviate its incomplete localization problem. The two modules interactively distill each other, forming a strong joint approach.

Our approach implements the state-of-the-art on two popular benchmarks, THUMOS14 and ActivityNet1.2. Furthermore, we find that our proposed approach can be applied to existing methods and improve their performance with significant advantages. Our contributions can be summarized in four aspects:

- We propose a paradigm, MLLM4WTAL, that guides WTAL methods using MLLM. To the best of our knowledge, this is the first work that enhances WTAL methods using MLLM. We also show that our method can be easily extended to existing state-of-the-art methods and improve their performance without introducing additional overhead in the inference phase.
- To fully leverage the prior information provided by MLLM, we design two modules, KSM and CSR, to enhance WTAL methods from the perspectives of key semantic matching and complete semantic reconstruction, respectively.
- To achieve a strong collaboration between KSM and CSR, we propose a dual prior interactive distillation strategy, cleverly addressing the incomplete and over-complete issues present in each module.
- Extensive experiments show that our method outperforms existing methods on two public datasets. Comprehensive ablation studies reveal the effectiveness of the proposed method.

Related Work

Temporal Action Localization requires the simultaneous prediction of action start and end times along with the corresponding category. In fully-supervised temporal action localization training, frame-level labeling is commonly em-

ployed. Existing methods fall into two main categories: top-down and bottom-up. Top-down methods (Chao et al. 2018; Gao et al. 2017) transform action localization into a time-dimensional detection task, inspired by image object detection. These methods generate action proposals, followed by classification and regression on temporal boundaries. They can draw on state-of-the-art techniques for Object Detection. On the other hand, bottom-up methods (Xu et al. 2020), (Bai et al. 2020) generate frame-level predictions, followed by action localization using cleverly designed post-processing techniques. However, this fully supervised approach relies heavily on frame-by-frame annotation, which is both expensive and impractical when dealing with long videos.

Weakly-Supervised Temporal Action Localization has garnered increasing attention within the research community, particularly due to its ability to learn from video-level category labels during training, thus circumventing the need for precise temporal annotations (Paul, Roy, and Roy-Chowdhury 2018; Narayan et al. 2021; Lee et al. 2021). The initial approach was UntrimmedNet (Wang et al. 2017), which first addressed this problem by employing a Multiple Instance Learning (MIL) framework that selects foreground segments and combines them into action segments. Subsequent improvement methods, such as STPN (Nguyen et al. 2018), enhanced UntrimmedNet by introducing a sparse loss to make the selected segments more sparse. CoLA (Zhang et al. 2021) utilizes contrastive learning to distinguish between foreground and background segments. In addition, UGCT (Yang et al. 2021) proposed an online pseudo-label generation mechanism with uncertainty-aware learning capability for pseudo-label supervision of attention weights.

Multimodal Large Language Models have emerged as a powerful paradigm for tackling a wide range of tasks spanning multiple modalities. LLM (Brown et al. 2020; Chiang et al. 2023; OpenAI 2023; Touvron et al. 2023) has recently excelled in Natural Language Processing (NLP) tasks. To integrate with other modalities, researchers have worked to construct MLLM (Li et al. 2023a,c; Zhu et al. 2023). Flamingo (Alayrac et al. 2022) integrates pre-trained visual and linguistic models to achieve state-of-the-art performance using a small number of samples. BLIP-2 (Li et al. 2023c) proposes a generic and efficient pre-training strategy that utilizes frozen pre-trained image encoders and large linguistic models for visual language pre-training. MiniGPT4 (Zhu et al. 2023) implements the system by aligning frozen visual coders and LLMs, Vicuna (Chiang et al. 2023), using only one projection layer. Otter (Li et al. 2023a) demonstrates improved instruction-following and context-learning capabilities. In the domain of video, ChatVideo (Wang et al. 2023) implements user interaction with LLMs using the tracklet as the fundamental video unit. VideoChat (Li et al. 2023d) integrates the video foundation models and LLMs through a learnable neural interface and performs well in spatio-temporal reasoning, event localization, and causal relationship inference. As for Video-LLaMA (Zhang, Li, and Bing 2023), it utilizes the pre-trained models ImageBind (Girdhar et al. 2023) and LLaMA (Touvron et al. 2023) on top of BLIP-2, which further facilitates cross-modal training for video.

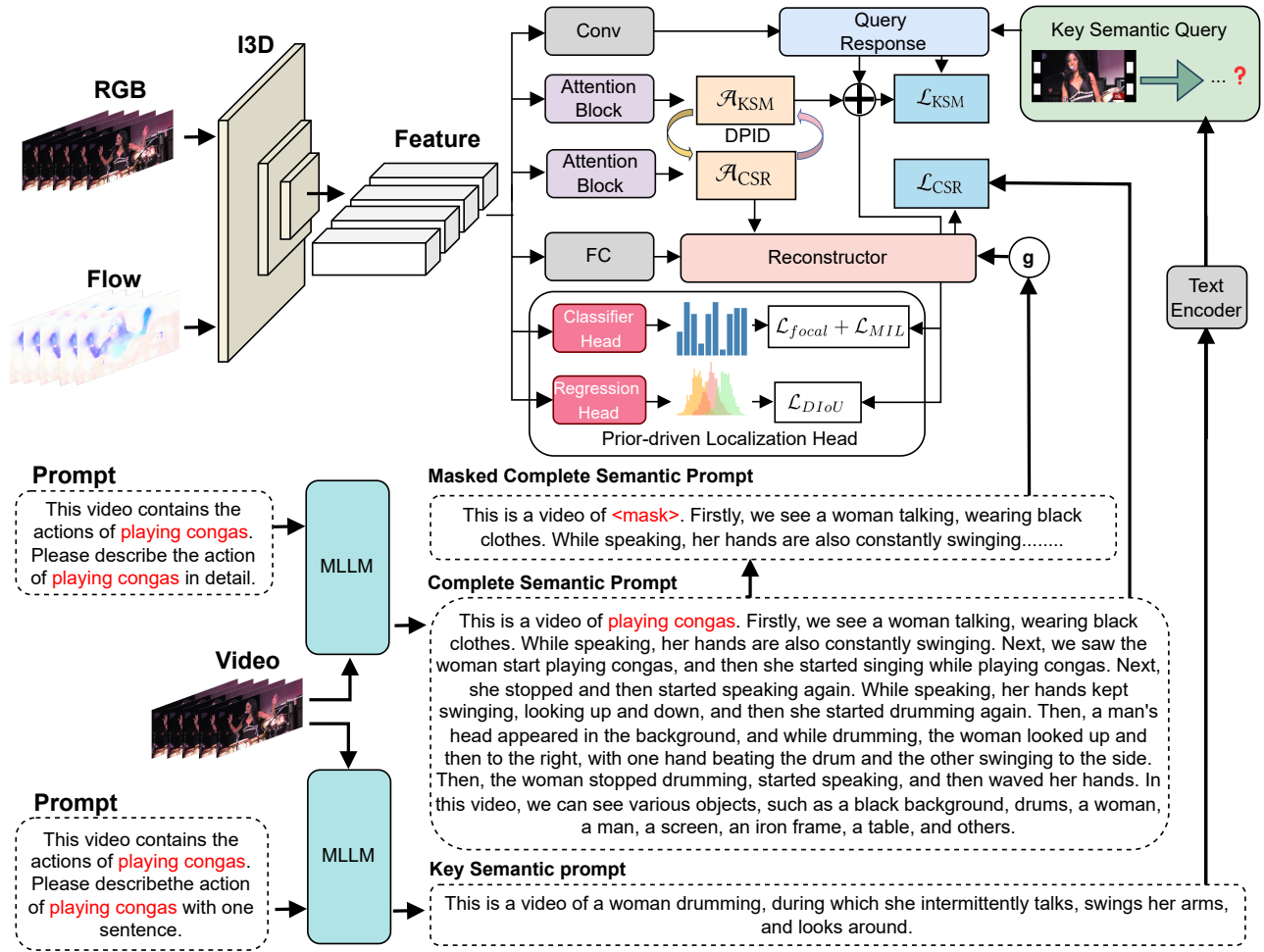


Figure 2: The overview of our method. In this work, Key Semantic Matching aims to mine critical temporal intervals of temporal actions in videos with the help of matching key semantics provided by MLLM with video segments. Complete Semantic Reconstruction aims to utilize the complete semantics provided by MLLM to reconstruct the complete semantics of masking key action words, thus mining as complete an action instance range as possible. The dual prior interactive distillation (DPID) between \mathcal{A}_{KSM} and \mathcal{A}_{CSR} achieves a powerful combination of Key Semantic Matching and Complete Semantic Reconstruction. Prior-driven Localization Head aims to refine pseudo-labels while avoiding the high computational overhead of using MLLM during inference.

Methods

Problem definition. Given an untrimmed video containing action instances from C categories, WTAL aims to predict a set of action instances $\{\phi \mid \phi_i = (c, q, t_s, t_e)\}$ using only video-level labels $y \in \{0, 1\}^C$. For each action instance, c represents the predicted category, q represents the confidence, and t_s and t_e represent the start timestamp and end timestamp, respectively.

Overview. The overall framework of proposed MLLM4WTAL is illustrated in Fig.2. It leverages the semantic priors of MLLM to enhance WTAL from two aspects: Key Semantic Matching (KSM) and Complete Semantic Reconstruction (CSR). The framework employs a dual priors interactive enhancement strategy to achieve interactive enhancement of these two semantic priors. For section , MLLM first takes the raw video input to

obtain a temporal action key description. Subsequently, the key semantic query prompt is constructed based on the prompt template and input to the text encoder to get the key semantic query. Then RGB and flow video features X_{rgb} and X_{flow} are fed into the video embedding module to generate video feature embedding. In the key semantic matching module, KSM matches the key semantic query with all video segments, obtaining a contrastive query response that activates the video segment most matching the key semantic. Additionally, attention weights are generated for each video segment to further suppress the response of background segments to the key semantic activation. For section , first MLLM inputs the raw video to get a complete description of the temporal action, then masks the sentence’s key action words. Next, the attention mechanism is designed to collect all the complete fragments associated

with the masked action words and predict the masked action words by a linguistic reconstructor. Finally, in section , a dual priors interactive enhancement strategy is employed to achieve a strong collaboration between KSM and CSR, aiming to obtain more accurate and complete localization results.

Key Semantic Matching

In this section, we will introduce key semantic matching (KSM) to comprehensively activate key temporal action intervals. Specifically, KSM consists of a key semantic generator, video embedding module, text embedding module, and semantic matching module. **Key Semantic Generator.** In the key semantic generator module, the first step is to construct key semantic prompts for MLLM, guiding the MLLM to generate key descriptions for temporal actions. It is worth noting that when building the prompts, we have prior knowledge of the action categories present in the video. We introduce this action category before our prompt template. The prompt template P_{key} format is as follows:

This video contains the actions of $\{Cls\}$. Please describe the action of $\{Cls\}$ with one sentence.

Input the prompt template P_{key} and the original video V into MLLM to get the key semantic description of the video D_{key} as:

$$D_{\text{key}} = \Phi_{\text{MLLM}}(P_{\text{key}}, V) \quad (1)$$

Video Embedding Module. Similar to other WTAL models, the video embedding module consists of two 1D convolutions followed by ReLU and Dropout layers. We adopt the same strategy as in (Bai et al. 2020) to fuse the RGB and flow features to obtain the input $F \in \mathbb{R}^{T \times 2048}$ of the video embedding module.

$$F = \Phi_{\text{fuse}}(F_{\text{rgb}}, F_{\text{flow}}) \quad (2)$$

The corresponding video feature embedding $F_e \in \mathbb{R}^{T \times 2048}$ can then be obtained by $F_e = \Phi_{\text{emb}}(F)$, where Φ_{emb} represents the video embedding module. In addition, following previous works (Hong et al. 2021; Islam, Long, and Radke 2021), an attention mechanism is used to generate attention weight $\mathcal{A}_{KSM} \in \mathbb{R}^{T \times 1}$ for each video clip.

$$\mathcal{A}_{KSM} = \text{sigmoid}(\Phi_{\text{attention}}(F_e)) \quad (3)$$

where $\Phi_{\text{attention}}$ is an attention mechanism containing some convolutional layers.

Text Embedding Module. The text embedding module aims to generate key semantic queries using key semantic descriptions. We have used the learnable prompt to obtain the input T_{query} for the text embedding module.

$$T_{\text{key}} = \Phi_{\text{GloVe}}(D_{\text{key}}) \quad (4)$$

$$T_{\text{query}} = [T_{\text{start}}, T_{\text{context}}, T_{\text{key}}], \quad (5)$$

where T_{start} represents the [START] token that was randomly initialized, T_{context} is the learnable textual context of length N_{context} , and T_{key} is the key informative textual feature embedded with GloVe (OpenAI 2023). Additionally, the $(C + 1)$ th additional context class embedding is initialized with 0. Subsequently, a transformer encoder, denoted

as Φ_{trans} , functions as the text embedding module to generate text queries. Importantly, it should be noted that the key semantic query F_{query} can be obtained through $F_{\text{query}} = \Phi_{\text{trans}}(T_{\text{query}})$, where $F_{\text{query}} \in \mathbb{R}^{(C+1) \times 2048}$.

Semantic Matching Module The semantic matching module aims to activate video segment features associated with key semantic queries. Specifically, we perform inner product operation on video embedding feature X_e and text embedding feature X_q to generate segment-level video-text similarity matrix $M \in \mathbb{R}^{T \times (C+1)}$. In addition to this, following (Hong et al. 2021; Islam, Long, and Radke 2021), we also employ the attention weight \mathcal{A}_{KSM} to suppress the background segment responses. The segment-level matching result $\hat{M} \in \mathbb{R}^{T \times (C+1)}$ for background suppression can be obtained by $\hat{M} = \mathcal{A}_{KSM} * M$, where $*$ denotes the element-wise multiplication. Following (Paul, Roy, and Roy-Chowdhury 2018; Min and Corso 2020), we employ top-k multi-instance learning to compute the matching loss. Specifically, we compute the average of top-k similarities on the time dimension of the response of a particular text query category as the video-level video-text similarity. For the j -th action category, the video-level similarities S_j and \hat{S}_j are generated from M and \hat{M} , respectively.

$$S_j = \max_{\substack{l \in \{1, \dots, T\} \\ |l|=k}} \frac{1}{k} \sum_{i \in l} M_i(j) \quad (6)$$

$$\hat{S}_j = \max_{\substack{l \in \{1, \dots, T\} \\ |l|=k}} \frac{1}{k} \sum_{i \in l} \hat{M}_i(j) \quad (7)$$

Where l is a set of indexes containing the top k segments with the highest similarity to the j -th text query, and k is the number of selected segments.

We then apply softmax to S_j and \hat{S}_j to generate video-level similarity scores p_j and \hat{p}_j .

$$p_j = \text{softmax}(S_j) \quad (8)$$

$$\hat{p}_j = \text{softmax}(\hat{S}_j) \quad (9)$$

We encourage positive scores for video-text category matching to approach 1, while negative scores for training KSM objectives should be close to zero.

Here, y_j and \hat{y}_j represent the video-text matching labels. In y_j , the additional $(C + 1)$ -th background class is labeled as 1, while in \hat{y}_j , it is labeled as 0. The L_{KSM} expression is as follows:

$$L_{KSM} = - \sum_{j=1}^{C+1} (y_j \log(p_j) + \hat{y}_j \log(\hat{p}_j)) \quad (10)$$

Complete Semantic Reconstruction

Complete Semantic Reconstruction aims to complete the masked keywords in video descriptions by focusing on as comprehensive as possible text-related video clips. The proposed CSR also contains a video embedding module and a text embedding module, in addition to the transformer reconstructor for multimodal interaction and reconstruction of the complete text description.

Complete Semantic Generator. In the Complete Semantic Generator module, we first need to construct MLLM complete semantic prompts that prompt the MLLM to generate complete information of action instance. It is worth noting that when constructing the cue, we know the action category that the video contains, and we introduce this action category a priori into our prompt cue template, which is formatted as follows:

This video contains the actions of Cls . Please describe the action of Cls in detail.

Enter the cue template P_{complete} and original video V into MLLM to get a description of the complete information of the video D_{complete}

$$D_{\text{complete}} = \Phi_{\text{MLLM}}(P_{\text{complete}}, V) \quad (11)$$

Video Embedding Module. Given the original video features $F \in \mathbb{R}^{T \times 2048}$, we obtain the corresponding video feature embedding $F_{\text{complete}} \in \mathbb{R}^{T \times 512}$ through a fully connected layer.

$$F_{\text{complete}} = \Phi_{\text{FC}}(F) \quad (12)$$

To explore the complete temporal intervals of video that are semantically related to text, CSR includes an attention mechanism similar to . The attention weights \mathcal{A}_{CSR} of the CSR module can be obtained through the following equation:

$$\mathcal{A}_{\text{CSR}} = \text{sigmoid}(\Phi_{\text{attention}}(F_e)) \quad (13)$$

where $\Phi_{\text{attention}}$ is an attention mechanism containing some convolutional layers.

Text Embedding Module. We mask the key action words of the video-complete description and embed the masked sentences with GloVe(Pennington, Socher, and Manning 2014) and a fully connected layer to obtain the complete semantic embedding $F_c \in \mathbb{R}^{m \times 512}$, where m is the length of the sentence.

Transformer Reconstructor. The Transformer reconstructor is used to reconstruct masked description sentences in the Complete Semantic Reconstruction module. First, Following (Zhai et al. 2020), we randomly mask 1/3 of the words in the sentence as alternative description sentences, which may lead to a high probability of masking action labeling text. Then, the transformer’s encoder is utilized to obtain foreground video features $F_{fg} \in \mathbb{R}^{T \times 512}$

$$\begin{aligned} F_{fg} &= \Phi_{\text{enc}}(F_{\text{complete}}, \mathcal{A}_{\text{CSR}}) \\ &= \delta \left(\frac{F_{\text{complete}} W_q (F_{\text{complete}} W_k)^T}{\sqrt{d_h}} * \mathcal{A}_{\text{CSR}} \right) F_{\text{complete}} W_v \end{aligned} \quad (14)$$

Where Φ_{enc} is the Transformer encoder, $\delta(\cdot)$ is the softmax function, $W_q, W_k, W_v \in \mathbb{R}^{512 \times 512}$ are the learnable parameters, and $d_h = 512$ is the feature dimension of F_{complete} .

The Transformer decoder is employed to obtain a multimodal representation $H \in \mathbb{R}^{m \times 512}$ to reconstruct masked sentences.

$$\begin{aligned} H &= \Phi_{\text{dec}}(F_c, F_{fg}, \mathcal{A}_{\text{CSR}}) \\ &= \delta \left(\frac{F_c W_{qd} (F_{fg} W_{kd})^T}{\sqrt{d_h}} * \mathcal{A}_{\text{CSR}} \right) F_{fg} W_{vd}, \end{aligned} \quad (15)$$

Where Φ_{dec} is the Transformer encoder, δ is the softmax function, $W_{qd}, W_{kd}, W_{vd} \in \mathbb{R}^{512 \times 512}$ are the learnable parameters.

Finally, the probability distribution of the i_{th} word w_i can be obtained by the following equation:

$$\mathbf{P}(w_i | F_{\text{complete}}, F_{c[0:i-1]}) = \text{sigmoid}(\Phi_{\text{FC}}(H)) \quad (16)$$

Where Φ_{FC} is the fully connected layer and N_v is the word size.

The final \mathcal{L}_{CSR} loss function is as follows:

$$\mathcal{L}_{\text{CSR}} = - \sum_{i=1}^m \log \mathbf{P}(w_i | F_{\text{complete}}, F_{\text{txt}[0:i-1]}) \quad (17)$$

Dual Prior Interactive Distillation

Following PivoTAL(Nayeem et al.), we utilized a prior-guided localization head. The loss function for the localization head is as follows:

$$\mathcal{L}_{\text{loc}} = \mathcal{L}_{\text{focal}} + \mathcal{L}_{\text{DIOU}} + \mathcal{L}_{\text{MIL}}. \quad (18)$$

The matching strategy employed in KSM tends to focus on better matching video segments that are crucial for describing the text, resulting in high true negatives but suffering from significant false negatives. On the other hand, CSR tends to focus on all video segments relevant to the complete text description to achieve complete description reconstruction, leading to high true positives but facing serious false positive issues. To address these challenges, an interactive distillation strategy is proposed to achieve a strong joint collaboration between the two branches.

The optimization process of the whole framework is divided into two phases, Key Semantic Matching and Complete Semantic Reconstruction, and the two phases are carried out alternately:

The loss function for the Key Semantic Matching phase is as follows:

$$\mathcal{L}_{\text{match}} = L_{\text{KSM}} + \lambda_1 \text{MSE}(\mathcal{A}_{\text{KSM}}, \psi(\mathcal{A}_{\text{CSR}})) + \mu_1 \mathcal{L}_{\text{loc}} \quad (19)$$

The loss function for the Complete Semantic Reconstruction phase is as follows:

$$\mathcal{L}_{\text{rec}} = \mathcal{L}_{\text{CSR}} + \lambda_2 \text{MSE}(\mathcal{A}_{\text{CSR}}, \psi(\mathcal{A}_{\text{KSM}})) \quad (20)$$

Interactive distillation optimization can encourage \mathcal{A}_{KSM} trained by KSM and \mathcal{A}_{CSR} trained by CSR to focus on the same action regions in the video. Through this strategy, it is possible to alleviate localization errors caused by the matching strategy’s excessive attention to the most relevant segments. In addition, the information of complete text description can be transferred from the Complete Semantic Reconstruction model to the WTAL model through the interactive distillation strategy.

Model Inference

During the training phase, we used MLLM to provide key semantics and complete semantic priors. However, during the inference phase, MLLM is no longer required, and only the prior-guided localization head needs to be executed, thus avoiding the significant computational overhead that could result from running MLLM

Sup	Method	Pub	mAP@IoU(%)							AVG		
			0.1	0.2	0.3	0.4	0.5	0.6	0.7	0.1:0.5	0.3:0.7	0.1:0.7
Full	SSN(Zhao et al. 2017)	ICCV2017	66.0	59.4	51.9	41	29.8	-	-	55.7	-	-
	P-GCN(Zeng et al. 2019)	CVPR2019	69.5	67.8	63.6	57.8	49.1	-	-	61.6	-	-
	G-TAD(Long et al. 2019)	CVPR2020	-	-	54.5	47.6	40.2	30.8	23.4	-	39.3	-
	ActionFormer(Zhang, Wu, and Li 2022)	ECCV2022	-	-	82.1	77.8	71.0	59.4	43.9	-	66.8	-
Weak	CoLA(Zhang et al. 2021)	CVPR2021	66.2	59.5	51.5	41.9	32.2	22.0	13.1	50.3	32.1	40.9
	DCC(Li et al. 2022)	CVPR2022	69.0	63.8	55.9	45.9	35.7	24.3	13.7	54.1	35.1	44.0
	Li et al.(Li et al. 2023b)	CVPR2023	71.1	65.0	56.2	47.8	39.3	27.5	15.2	55.9	37.2	46.0
	Wang et al.(Wang, Li, and Wang)	CVPR2023	73.0	68.2	60.0	47.9	37.1	24.4	12.7	57.2	36.4	46.2
	Ren et al.(Ren et al. 2023)	CVPR2023	71.8	67.5	58.9	49.0	40.0	27.1	15.1	57.4	38.0	47.1
	STCL-Net(Fu, Gao, and Xu)	TPAMI2023	72.7	67.1	58.2	49.7	41.8	28.7	16.0	57.9	38.9	47.7
	Ju et al.(Liu et al. b)	CVPR2023	73.5	68.8	61.5	53.8	42.0	29.4	16.8	59.9	40.7	49.4
	PivoTAL(Nayeem et al.)	CVPR2023	74.1	69.6	61.7	52.1	42.8	30.6	16.7	60.1	40.8	49.7
	AHLM(AHL 2023)	ICCV2023	75.1	68.9	60.2	48.9	38.3	26.8	14.7	58.3	37.8	47.6
	CASE(Liu et al. a)	ICCV2023	72.3	67.1	59.2	49.4	37.7	24.2	13.7	57.1	36.8	46.2
	ISSF(Yun et al. 2023)	AAAI2024	72.4	66.9	58.4	49.7	41.8	25.5	12.8	57.8	37.6	46.8
	DELU(Chen et al. 2022)	ECCV2022	71.5	66.2	56.5	47.7	40.5	27.2	15.3	56.5	37.4	46.4
	MLLM4WTAL (DELU)	-	72.3	67.0	57.3	48.2	42.4	29.7	18.4	57.4	39.2	47.9
	Zhou et al.(Zhou et al. 2023)	CVPR2023	74.0	69.4	60.7	51.8	42.7	26.2	13.1	59.7	38.9	48.3
	MLLM4WTAL (Zhou et al.)	-	74.3	69.8	61.8	52.3	43.0	30.8	16.6	61.7	40.9	49.8

Table 1: Experimental results of different methods in THUMOS14 dataset

Method	Pub	mAP(%)@IoU			Avg
		0.5	0.75	0.95	
CoLA(Zhang et al. 2021)	CVPR2021	42.7	25.7	5.8	26.1
ACGNet(Lee et al. 2021)	AAAI2022	41.8	26.0	5.9	26.1
DGCNN(Shi et al. 2022)	MM2022	42.0	25.8	6.0	26.2
P-MIL(Ren et al. 2023)	CVPR2023	44.2	26.1	5.3	26.5
ECM(Zhao et al. 2022)	TPAMI2023	41.0	24.9	6.5	25.5
Ren et al.(Ren et al. 2023)	CVPR2023	44.2	26.1	5.3	25.5
STCL-Net(Fu, Gao, and Xu)	TPAMI2023	44.0	26.1	5.3	26.6
Ju et al.(Liu et al. b)	CVPR2023	48.3	29.3	6.1	29.6
CASE(Liu et al. a)	ICCV2023	43.8	27.2	6.7	27.9
DELU(Chen et al. 2022)	ECCV2022	44.2	26.7	5.4	26.8
MLLM4WTAL (DELU)	-	45.0	28.1	6.1	28.9
DDG-Net(Tang et al.)	ICCV2023	44.3	26.9	5.5	27.0
MLLM4WTAL (DDG-Net)	-	48.3	30.1	6.8	30.1

Table 2: Experimental results of different methods in ActivityNet-v1.2 dataset

Method	mAP(%)@IoU					Avg
	0.3	0.4	0.5	0.6	0.7	
Baseline	56.5	47.7	40.5	27.2	15.3	37.4
Baseline+KSM	56.8	47.9	41.9	28.8	17.7	38.9
Baseline+CSR	56.9	47.8	41.7	28.6	17.5	38.7
Baseline+KSM+CSR	57.3	48.2	42.4	29.7	18.4	39.2

Table 3: Evaluation of each component of our method

Experiment

In this section, we first show the dataset and implementation details and then compare our approach with recent state-of-the-art methods. Next, we perform a series of ablation studies to validate the effectiveness of our proposed components. In addition to this, we perform a generalization validation of our MLLM4WTAL framework. Finally, qualitative analyses are presented at the end of this section.

Method	KSM	CSR	mAP(%)@IoU			Avg
			0.3	0.5	0.7	
UM(Lee et al. 2021)	✓		51.2	30.4	10.2	30.3
	✓	✓	52.4	33.0	12.5	32.1
CO2-Net(Hong et al. 2021)	✓		54.8	38.4	13.8	36.0
	✓	✓	55.9	40.8	16.6	37.9
			56.2	41.3	17.5	38.2

Table 4: Generic validation of our method

THUMOS14(Idrees et al. 2017) contains 413 untrimmed videos covering 20 different categories of actions. On average, each video contains about 15 unique instances of actions. We trained using 200 validation videos and evaluated on 213 test videos. Despite the small size of the dataset, it is challenging because the videos vary greatly in length and action instances occur more frequently in each video.

ActivityNet-v1.2(Caba Heilbron et al. 2015) covers 9682 videos that include 100 different classes of actions. These videos were categorized into 4619 training videos, 2383 validation videos, and 2480 test videos. Almost all of the videos contain at least one action category, and the action duration usually occupies more than half of the video duration. We performed model training on the training set and performance evaluation on the validation set.

Evaluation metrics. Following the standard protocol for temporal action localization [6], we chose the mean accuracy at different intersection-union ratio (IoU) thresholds (mAP@IoU) to evaluate the model performance. For a fair comparison, we use an IoU threshold range of [0.1:0.1:0.7] on the THUMOS-14 dataset and an IoU threshold range of [0.5:0.05:0.95] on ActivityNet-v1.2. The official evaluation code provided by ActivityNet is used to assess the model’s performance(Caba Heilbron et al. 2015).

Training Settings. We employed the Adam optimizer with a learning rate of 0.0005 and a weight decay of 0.001 for approximately 5,000 iterations to train the model on the THUMOS14 dataset. On ActivityNet-v1.2, the learning rate was set to 0.00003 for model optimization across 50,000 iterations. Additionally, λ_1 , λ_2 , μ_1 were set sequentially to 1.50, 1.50, 1.00 (Detailed hyperparameter analysis can be found in the supplementary materials). The implementation of our model was based on PyTorch 1.8, and training was conducted on the Ubuntu 18.04 platform.

Comparison with State-of-the-art Methods.

In this section, we compare our proposed method with the current state-of-the-art temporal action localization methods, as presented in Tables 1 and 2. For the THUMOS14 dataset, we selected DELU and Zhou et al. (Zhou et al. 2023) as our baseline methods. After incorporating our MLLM4WTAL, we achieved improvements of 1.8% and 1.0% in the average mAP (0.1:0.7) metric, respectively, surpassing current weakly supervised methods and even outperforming some fully supervised methods, such as SSN, P-GCN, and G-TAD. On the larger-scale ActivityNet-v1.2 dataset, our method achieves a 0.5% improvement in average mAP compared to existing state-of-the-art methods.

Ablation Study

To analyze the contribution of each of our proposed modules, we conducted extensive ablation experiments to evaluate our approach from multiple perspectives, as shown in 3.

Baseline: In the baseline experimental setup, without using any of our proposed components, we achieved an average mAP of 37.4%.

Impact of KSM: In the Baseline+KSM experimental setup, where we solely incorporated the proposed Key Semantic Matching (KSM), we achieved an average mAP of 38.9%. The introduction of KSM resulted in a more significant mAP improvement, especially in high IoU settings. For instance, at IoU=0.7, there was a relative improvement of 1.6% compared to the Baseline.

Impact of CSR: In the Baseline+CSR experimental setup, where only the proposed Complete Semantic Reconstruction (CSR) was utilized, we achieved an average mAP of 38.7%. Similar to KSM, the introduction of CSR led to a more pronounced mAP improvement, with a relative increase of 2.2% at IoU=0.7 compared to the Baseline.

Combined Impact of KSM and CSR: In the Baseline+KSM+CSR experimental setup, where both KSM and CSR were simultaneously employed, we achieved an average mAP of 39.2%. The simultaneous introduction of KSM and CSR resulted in a more noticeable mAP improvement, particularly in high IoU settings. For example, at IoU=0.7, there was a relative improvement of 3.1% compared to the Baseline.

Generic validation

It is important to emphasize the versatility of our MLLM4WTAL framework, as it can be plug-and-played

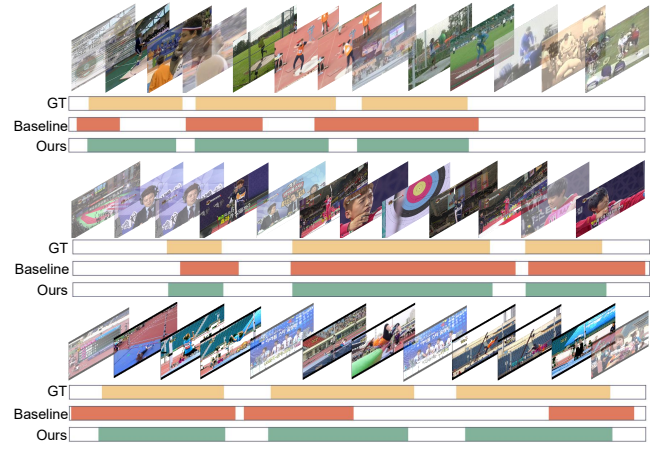


Figure 3: Visualization of ground-truth and predictions.

into existing mainstream WTAL methods. To assess the generality of our framework, we systematically incorporated two classical WTAL methods, UM and CO2-Net, into our framework. Utilizing only UM resulted in an average mAP of 30.3%, and subsequent integration of KSM and CSR led to average mAP improvements of 1.8% and 2.3%, respectively. Similarly, employing only CO2-Net yielded an average mAP of 36.0%, with sequential addition of KSM and CSR resulting in average mAP enhancements of 1.9% and 2.2%, respectively. These findings robustly demonstrate the adaptability of our method in effectively enhancing various mainstream WTAL methods.

Qualitative Analysis

As shown in Fig.3, we present the visual results of temporal action localization. From the visualization, it can be observed that the baseline exhibits significant issues of over-complete and incomplete localization results. However, upon introducing our MLLM, which provides key semantic and complete semantic priors, the problems of over-complete and incomplete are noticeably alleviated.

Conclusion

We introduce a paradigm, MLLM4WTAL, to guide the Weakly-supervised Temporal Action Localization (WTAL) task. The MLLM4WTAL framework enhances the WTAL methods in two ways: Key Semantic Matching and Complete Semantic Reconstruction. Key Semantic Matching aims to utilize the key semantic priors provided by MLLM to activate crucial intervals of action instances. Complete Semantic Reconstruction aims to leverage the complete semantic priors provided by MLLM to mine as complete action instance intervals as possible. Integrating the prediction results of the above two modules, a dual prior interactive distillation strategy is employed to address the common issues of over-complete and incomplete in WTAL. Extensive experiments demonstrate that our approach achieves state-of-the-art performance on two popular datasets and can be plug-and-played into existing WTAL methods.

References

2023. Weakly-Supervised Action Localization by Hierarchically-structured Latent Attention Modeling.
- Alayrac, J.-B.; Donahue, J.; Luc, P.; Miech, A.; Barr, I.; Hasson, Y.; Lenc, K.; Mensch, A.; Millican, K.; Reynolds, M.; et al. 2022. Flamingo: a visual language model for few-shot learning. *Advances in Neural Information Processing Systems*, 35: 23716–23736.
- Bai, Y.; Wang, Y.; Tong, Y.; Yang, Y.; Liu, Q.; and Liu, J. 2020. Boundary content graph neural network for temporal action proposal generation. In *Computer Vision—ECCV 2020: 16th European Conference, Glasgow, UK, August 23–28, 2020, Proceedings, Part XXVIII 16*, 121–137. Springer.
- Brown, T.; Mann, B.; Ryder, N.; Subbiah, M.; Kaplan, J. D.; Dhariwal, P.; Neelakantan, A.; Shyam, P.; Sastry, G.; Askell, A.; et al. 2020. Language models are few-shot learners. *Advances in neural information processing systems*, 33: 1877–1901.
- Caba Heilbron, F.; Escorcia, V.; Ghanem, B.; and Carlos Niebles, J. 2015. Activitynet: A large-scale video benchmark for human activity understanding. In *Proceedings of the IEEE conference on computer vision and pattern recognition*, 961–970.
- Chao, Y. W.; Vijayanarasimhan, S.; Seybold, B.; Ross, D. A.; Deng, J.; and Sukthankar, R. 2018. Rethinking the Faster R-CNN Architecture for Temporal Action Localization. In *2018 IEEE/CVF Conference on Computer Vision and Pattern Recognition*.
- Chen, M.; Gao, J.; Yang, S.; and Xu, C. 2022. Dual-evidential learning for weakly-supervised temporal action localization. In *European Conference on Computer Vision*, 192–208. Springer.
- Chiang, W.-L.; Li, Z.; Lin, Z.; Sheng, Y.; Wu, Z.; Zhang, H.; Zheng, L.; Zhuang, S.; Zhuang, Y.; Gonzalez, J. E.; et al. 2023. Vicuna: An open-source chatbot impressing gpt-4 with 90%* chatgpt quality. See <https://vicuna.lmsys.org> (accessed 14 April 2023).
- Dai, W.; Li, J.; Li, D.; Tiong, A.; Zhao, J.; Wang, W.; Li, B.; Fung, P.; and Hoi, S. ????. InstructBLIP: Towards General-purpose Vision-Language Models with Instruction Tuning. *arXiv 2023. arXiv preprint arXiv:2305.06500*.
- Fu, J.; Gao, J.; and Xu, C. ????. Semantic and Temporal Contextual Correlation Learning for Weakly-Supervised Temporal Action Localization.
- Gao, J.; Yang, Z.; Sun, C.; Chen, K.; and Nevatia, R. 2017. TURN TAP: Temporal Unit Regression Network for Temporal Action Proposals. *IEEE*.
- Girdhar, R.; El-Nouby, A.; Liu, Z.; Singh, M.; Alwala, K. V.; Joulin, A.; and Misra, I. 2023. Imagebind: One embedding space to bind them all. In *Proceedings of the IEEE/CVF Conference on Computer Vision and Pattern Recognition*, 15180–15190.
- Hong, F.-T.; Feng, J.-C.; Xu, D.; Shan, Y.; and Zheng, W.-S. 2021. Cross-modal consensus network for weakly supervised temporal action localization. In *Proceedings of the 29th ACM international conference on multimedia*, 1591–1599.
- Idrees, H.; Zamir, A. R.; Jiang, Y.-G.; Gorban, A.; Laptev, I.; Sukthankar, R.; and Shah, M. 2017. The thumos challenge on action recognition for videos “in the wild”. *Computer Vision and Image Understanding*, 155: 1–23.
- Islam, A.; Long, C.; and Radke, R. 2021. A hybrid attention mechanism for weakly-supervised temporal action localization. In *Proceedings of the AAAI Conference on Artificial Intelligence*, volume 35, 1637–1645.
- Lee, P.; Wang, J.; Lu, Y.; and Byun, H. 2021. Weakly-supervised temporal action localization by uncertainty modeling. In *Proceedings of the AAAI conference on artificial intelligence*, volume 35, 1854–1862.
- Li, B.; Zhang, Y.; Chen, L.; Wang, J.; Yang, J.; and Liu, Z. 2023a. Otter: A multi-modal model with in-context instruction tuning. *arXiv preprint arXiv:2305.03726*.
- Li, G.; Cheng, D.; Ding, X.; Wang, N.; Wang, X.; and Gao, X. 2023b. Boosting weakly-supervised temporal action localization with text information. In *Proceedings of the IEEE/CVF Conference on Computer Vision and Pattern Recognition*, 10648–10657.
- Li, J.; Li, D.; Savarese, S.; and Hoi, S. 2023c. Blip-2: Bootstrapping language-image pre-training with frozen image encoders and large language models. *arXiv preprint arXiv:2301.12597*.
- Li, J.; Yang, T.; Ji, W.; Wang, J.; and Cheng, L. 2022. Exploring denoised cross-video contrast for weakly-supervised temporal action localization. In *Proceedings of the IEEE/CVF Conference on Computer Vision and Pattern Recognition*, 19914–19924.
- Li, K.; He, Y.; Wang, Y.; Li, Y.; Wang, W.; Luo, P.; Wang, Y.; Wang, L.; and Qiao, Y. 2023d. Videochat: Chat-centric video understanding. *arXiv preprint arXiv:2305.06355*.
- Liu, Q.; Wang, Z.; Rong, S.; Li, J.; and Zhang, Y. ????.a. Re-visiting Foreground and Background Separation in Weakly-supervised Temporal Action Localization: A Clustering-based Approach.
- Liu, Y.; Xio, Z.; Yuan, Y.; and Wang, Q. ????.b. Distilling Knowledge From Super-Resolution for Efficient Remote Sensing Salient Object Detection.
- Long, F.; Yao, T.; Qiu, Z.; Tian, X.; Luo, J.; and Mei, T. 2019. Gaussian temporal awareness networks for action localization. In *Proceedings of the IEEE/CVF conference on computer vision and pattern recognition*, 344–353.
- Min, K.; and Corso, J. J. 2020. Adversarial background-aware loss for weakly-supervised temporal activity localization. In *Computer Vision—ECCV 2020: 16th European Conference, Glasgow, UK, August 23–28, 2020, Proceedings, Part XIV 16*, 283–299. Springer.
- Narayan, S.; Cholakkal, H.; Hayat, M.; Khan, F. S.; Yang, M.-H.; and Shao, L. 2021. D2-net: Weakly-supervised action localization via discriminative embeddings and denoised activations. In *Proceedings of the IEEE/CVF International Conference on Computer Vision*, 13608–13617.
- Nayeem, M.; Mittal, G.; Yu, Y.; Hall, M.; Sajeev, S.; Shah, M.; Chen, M.; and Microsoft. ????. PivoTAL: Prior-Driven Supervision for Weakly-Supervised Temporal Action Localization.

- Nguyen, P.; Liu, T.; Prasad, G.; and Han, B. 2018. Weakly supervised action localization by sparse temporal pooling network. In *Proceedings of the IEEE conference on computer vision and pattern recognition*, 6752–6761.
- OpenAI. 2023. GPT-4 Technical Report. Technical report.
- Paul, S.; Roy, S.; and Roy-Chowdhury, A. K. 2018. W-talc: Weakly-supervised temporal activity localization and classification. In *Proceedings of the European Conference on Computer Vision (ECCV)*, 563–579.
- Pennington, J.; Socher, R.; and Manning, C. D. 2014. Glove: Global vectors for word representation. In *Proceedings of the 2014 conference on empirical methods in natural language processing (EMNLP)*, 1532–1543.
- Ren, H.; Yang, W.; Zhang, T.; and Zhang, Y. 2023. Proposal-Based Multiple Instance Learning for Weakly-Supervised Temporal Action Localization. In *Proceedings of the IEEE/CVF Conference on Computer Vision and Pattern Recognition*, 2394–2404.
- Shi, H.; Zhang, X.-Y.; Li, C.; Gong, L.; Li, Y.; and Bao, Y. 2022. Dynamic Graph Modeling for Weakly-Supervised Temporal Action Localization. In *Proceedings of the 30th ACM International Conference on Multimedia*, 3820–3828.
- Tang, X.; Fan, J.; Luo, C.; Zhang, Z.; Zhang, M.; and Yang, Z. ????. DDG-Net: Discriminability-Driven Graph Network for Weakly-supervised Temporal Action Localization.
- Touvron, H.; Martin, L.; Stone, K.; Albert, P.; Almahairi, A.; Babaei, Y.; Bashlykov, N.; Batra, S.; Bhargava, P.; Bhosale, S.; et al. 2023. Llama 2: Open foundation and fine-tuned chat models. *arXiv preprint arXiv:2307.09288*.
- Wang, J.; Chen, D.; Luo, C.; Dai, X.; Yuan, L.; Wu, Z.; and Jiang, Y.-G. 2023. Chatvideo: A tracklet-centric multimodal and versatile video understanding system. *arXiv preprint arXiv:2304.14407*.
- Wang, L.; Xiong, Y.; Lin, D.; and Van Gool, L. 2017. Untrimmednets for weakly supervised action recognition and detection. In *Proceedings of the IEEE conference on Computer Vision and Pattern Recognition*, 4325–4334.
- Wang, Y.; Li, Y.; and Wang, H. ????. Two-Stream Networks for Weakly-Supervised Temporal Action Localization with Semantic-Aware Mechanisms.
- Xu, M.; Zhao, C.; Rojas, D. S.; Thabet, A.; and Ghanem, B. 2020. G-tad: Sub-graph localization for temporal action detection. In *Proceedings of the IEEE/CVF conference on computer vision and pattern recognition*, 10156–10165.
- Yang, W.; Zhang, T.; Yu, X.; Qi, T.; Zhang, Y.; and Wu, F. 2021. Uncertainty guided collaborative training for weakly supervised temporal action detection. In *Proceedings of the IEEE/CVF Conference on Computer Vision and Pattern Recognition*, 53–63.
- Yun, W.; Qi, M.; Wang, C.; and Ma, H. 2023. Weakly-Supervised Temporal Action Localization by Inferring Salient Snippet-Feature.
- Zeng, R.; Huang, W.; Tan, M.; Rong, Y.; Zhao, P.; Huang, J.; and Gan, C. 2019. Graph convolutional networks for temporal action localization. In *Proceedings of the IEEE/CVF international conference on computer vision*, 7094–7103.
- Zhai, Y.; Wang, L.; Tang, W.; Zhang, Q.; Yuan, J.; and Hua, G. 2020. Two-stream consensus network for weakly-supervised temporal action localization. In *Computer Vision–ECCV 2020: 16th European Conference, Glasgow, UK, August 23–28, 2020, Proceedings, Part VI 16*, 37–54. Springer.
- Zhang, C.; Cao, M.; Yang, D.; Chen, J.; and Zou, Y. 2021. Cola: Weakly-supervised temporal action localization with snippet contrastive learning. In *Proceedings of the IEEE/CVF Conference on Computer Vision and Pattern Recognition*, 16010–16019.
- Zhang, C.-L.; Wu, J.; and Li, Y. 2022. Actionformer: Localizing moments of actions with transformers. In *European Conference on Computer Vision*, 492–510. Springer.
- Zhang, H.; Li, X.; and Bing, L. 2023. Video-llama: An instruction-tuned audio-visual language model for video understanding. *arXiv preprint arXiv:2306.02858*.
- Zhao, T.; Han, J.; Yang, L.; and Zhang, D. 2022. Equivalent classification mapping for weakly supervised temporal action localization. *IEEE transactions on pattern analysis and machine intelligence*, 45(3): 3019–3031.
- Zhao, Y.; Xiong, Y.; Wang, L.; Wu, Z.; Tang, X.; and Lin, D. 2017. Temporal action detection with structured segment networks. In *Proceedings of the IEEE international conference on computer vision*, 2914–2923.
- Zhou, J.; Huang, L.; Wang, L.; Liu, S.; and Li, H. 2023. Improving weakly supervised temporal action localization by bridging train-test gap in pseudo labels. In *Proceedings of the IEEE/CVF Conference on Computer Vision and Pattern Recognition*, 23003–23012.
- Zhu, D.; Chen, J.; Shen, X.; Li, X.; and Elhoseiny, M. 2023. Minigpt-4: Enhancing vision-language understanding with advanced large language models. *arXiv preprint arXiv:2304.10592*.